Raytheon

LITTORAL SEDIMENT TRANSPORT

VISIBLE/INFRARED IMAGER/RADIOMETER SUITE ALGORITHM THEORETICAL BASIS DOCUMENT

Version 4: May 2001

Caitlin P. Mullen
Alexander P. Vasilkov

Dorlisa Hommel
Raymond Smith, Science Team Member
University of California, Santa Barbara
Kendall Carder, Science Team Member
University of South Florida

RAYTHEON SYSTEMS COMPANY
Information Technology and Scientific Services
4400 Forbes Boulevard
Lanham, MD 20706

SBRS Document #: Y2406

EDR: Littoral Sediment Transport (40.7.4)

Doc No: Y2406
Version: 4
Revision: 0

	FUNCTION	NAME	SIGNATURE	DATE
PREPARED BY	EDR DEVELOPER	C. MULLEN A. VASILKOV		4/25/00
APPROVED BY	RELEVANT LEAD	D. HOMMEL		
APPROVED BY	CHIEF SCIENTIST	S. MILLER		
RELEASED BY	ALGORITHM IPT LEAD	P. KEALY		

TABLE OF CONTENTS

Page

LIST OF FIGURES

Page

GLOSSARY OF ACRONYMS

ATBD	Algorithm Theoretical Basic Document
Case 1	Water whose optically-active constituents are totally correlated
Case 2	Water whose optically-active constituents are not totally correlated
COIS	Coastal Ocean Imaging Spectrometer
CDOM	Colored Dissolved Organic Matter
DAAC	Data Analysis and Archive Center
DOM	Dissolved Organic Matter
EDR	Environmental Data Record
GSFC	NASA Goddard Space Flight Center
IOP	Inherent Optical Properties
LST	Littoral Sediment Transport
MAS	MODIS Airborne Simulator
MODIS	Moderate Resolution Imaging Spectrometer
NPOESS	National Polar-orbiting Operational Environmental Satellite System
RT	Radiative Transfer
SPM	Suspended Particulate Matter
TOA	Top of the Atmosphere
VIIRS	Visible/Infrared Imager/Radiometer Suite

GLOSSARY OF SYMBOLS

a	Absorption coefficient
A	Cell area
b_b	Backscattering coefficient
C	Chlorophyll *a* concentration
E	Irradiance
h	Water depth
k	DOM spectral absorption slope
L_w	Water-leaving radiance
n	Seawater refractive index
Q	Q-factor
R	Diffuse reflectance, i.e., the ratio of the upwelling irradiance to the downwelling irradiance just beneath the sea surface
R_{rs}	Remote-sensing reflectance, i.e., the ratio of water-leaving radiance to the downwelling irradiance just above the sea surface
S_i	Free parameters
λ	Wavelength
θ	Zenith angle

ABSTRACT

Littoral sediment transport is defined as the change in the volume of sediment on the floor of a river or the ocean in the cell since the last measurement, divided by the time interval between measurements. This definition suggests an optical bathymetry approach using the semi-transparent properties of seawater near 500 nm. Sequential retrievals of depth in coastal waters would be differenced to estimate sediment transport. Optical bathymetry relies on the detection of reflected radiation from the bottom, with a signal strength that decreases exponentially with increasing depth. As a result, bathymetry techniques are limited to optically shallow waters (Secchi depth < bottom depth) under low-turbidity conditions, with a practical limit of about 20 meters depth.

Major error sources for an optical bathymetry approach to estimating littoral sediment transport include the atmospheric correction, spatial variability of depth within the sensor field-of-view, uncertainty in the bottom reflectance, variations in chlorophyll concentration, and suspended sediment.

The littoral sediment transport algorithm makes use of the VIIRS visible bands at 555 and 672 nm. Assuming that bottom relfectance does not change during sequential measurements, the algorithm retrieves bottom depth changes from remote sensing reflectance at 555nm. The bottom depth changes are directly related to LST values through a cell area and time elasped between two sequential measurements. The red band at 672 nm is used in accounting for possible changes to the water turbidity during the sequential measurements. Evaluation of the algorithm and sensitivity studies was done using simulated datasets. Simulations of remote sensing relfectance were carried out using the HYDROLIGHT software. The simulations have shown that the algorithm is capable of meeting the SRD thresholds only for a variety ofenvironmental conditions.

An alternative approach to determining the littoral sediment transport EDR product is to create a time series of measurements. This technique is especially useful if the customer is interested in littoral sediment transport tendencies, as opposed to real-time operational information.

1.0 INTRODUCTION

1.1 PURPOSE

This Algorithm Theoretical Basis Document (ATBD) describes the algorithms used to determine the VIIRS Littoral Sediment Transport (LST) Product, a category-three product of the Visible/Infrared Imager/Radiometer Suite (VIIRS). Littoral Sediment Transport is measured in m^3/day units and retrieved from remote sensing reflectances. In particular, this document identifies sources of input data, both VIIRS and non-VIIRS, that are required for Littoral Sediment Transport retrievals; provides the physical theory and mathematical background underlying the use of this information in the retrievals; includes implementation details; and describes assumptions and limitations of the adopted approach.

1.2 SCOPE

This document covers the algorithm theoretical basis for the retrieval LST from remote sensing reflectances. Section 1 describes the purpose and scope of the document. Section 2 provides an experiment overview. The processing concept and algorithm descriptions are presented in Section 3. Section 4 summarizes the assumptions and limitations. References for publications cited in the text are given in Section 5.

1.3 VIIRS DOCUMENTS

A number in italicized brackets indicates references to VIIRS documents.

[V-1]	VIIRS Experiment Overview
[V-2]	Atmospheric Correction over Ocean
[V-3]	Visible/Infrared Imager Radiometer Suite (VIIRS) Payload and Algorithm Development for NPOESS, Vol II. Technical/Management Approaches Publication No. 97-0096,1997.
[V-4]	VIIRS Sensor Requirements Document, Technical Requirements Document, 1997.

1.4 REVISIONS

The original version of this document was dated July 23, 1998. Version 2 is dated June 1999. Version 3 is dated May 2000. In version 3 results were updated and additions were made to the retrieval strategy, background, and theoretical description sections. This is the fourth version of this document, dated May 2001. A minor revision was made to the VIIRS Data section.

2.0 EXPERIMENT OVERVIEW

2.1 OBJECTIVES OF LITTORAL SEDIMENT TRANSPORT RETRIEVALS

The required Environmental Data Record (EDR) is the transport of deposited, bottom-lying sediment in ocean coastal areas by river systems and along-shore ocean currents *[V-4]*. More specifically, it is defined as the change in the volume of sediment on the floor of the ocean in a horizontal cell in an ocean coastal area since the last measurement divided by the time interval between measurements.

Ocean waves begin to feel the seafloor, as they get closer to the coast. The interaction with the seabed results in the movement of bottom sediment. This movement changes the bathymetry of the littoral ocean floor, which in turn affects the arrival of the incoming waves. Thus, the littoral region is an area of intense dynamics where there is continued change in the bathymetry, wave, and current patterns.

In addition to the waves that continually affect the littoral regions, rip currents, edge waves, and shear waves are also present. Longshore currents and rip currents are the major components of the circulation cell within the coastal zone. Longshore currents cause the transport of sand alongshore, while rip currents are responsible for the cross-shore sediment transport. Burns (1998) points out that these larger-scale currents and waves play a major role in the configuration of the littoral region. This is shown by the fact that the variability and scale of the offshore bars are greater than that for the breaking waves (Burns, 1998). These bars can undergo changes within days (or less) of an offshore event.

Military personnel are extremely interested in the dynamics and morphological changes of the littoral region. Equipment-laden troops can drown in the deep troughs near sandbars. Intense wave activity within the coastal zone can greatly affect the maneuvering of amphibious craft. Channels within the sand, and the rapid currents they can contain, can affect the approach of the craft, swimmers, and torpedoes. For both the Navy and the Marine Corps, therefore, a thorough understanding of the coastal topography, oceanography, and meteorology is paramount to the success of their missions. The key element of amphibious assaults and SEAL operations is the ability to maneuver vehicles and personnel from the sea through the coastal zone to the land. But the beach profile and the littoral zone are constantly changing. The sand profile changes seasonally, and it changes dramatically during and after storm events. Barred beaches with rip currents are very common. Therefore, an understanding of the transport and deposition of sediment within the littoral zone is essential for military operations.

Storms, seasonal changes, coastal currents, waves, and other coastal phenomena affect the rate of sedimentation and sediment transport within the littoral zone and sediment deposition plays a key role in mine warfare. The capability to monitor the change in bathymetry (i.e., the sedimentation rate in the littoral zone) over time enables military personnel to detect and locate underwater mines and develop different mine warfare systems.

Knowledge of littoral processes such as sediment deposition and transportation is also very important for economic reasons, as well as for navigation, channel shoaling control, pollution tracking, and ocean engineering.

The overall scientific objectives of the VIIRS littoral sediment transport retrievals are:

- To determine short-term changes in water depth in the shallow coastal oceans due to sediment transport events;

- To study, on a global basis, the magnitude and natural variability in space and time of sediment transport events in the coastal zone, particularly through determination of shallow water bathymetry using passive optical techniques; and

- To provide improved measures of coastal zone processes and dynamics in conjunction with other VIIRS ocean EDRs.

The scientific background for each of these objectives, a historical perspective on retrievals using remote sensing, the unique contribution of VIIRS, and the scientific rationale for the contents of the VIIRS Littoral Sediment Transport Product are presented in *[V-1]*.

2.2 INSTRUMENT CHARACTERISTICS

The retrieval of ocean EDRs is based on algorithms using the spectral reflectance of the seawater column in the visible spectral region. VIIRS has five spectral bands in the visible region *[V-1]*. Their centers are located at wavelengths 413, 443, 488, 555, and 672 nm. Bandwidths are equal to 20 nm.

2.3 RETRIEVAL STRATEGY

Littoral sediment transport is defined as the change in the volume of sediment on the floor of a river or the ocean in the specified horizontal cell since the last measurement, divided by the time interval between measurements. This definition suggests an optical bathymetry approach utilizing the semi-transparent properties of water near 500 nm. Sequential retrievals of depth in coastal waters would be compared to estimate sediment transport. Optical bathymetry relies on the detection of reflected radiation from the bottom, with a signal strength that decreases exponentially with increasing water depth. As a result, bathymetry techniques are limited to optically shallow waters (Secchi depth < bottom depth) under low-turbidity conditions, with a practical depth limit of about 10 meters. Major error sources for an optical bathymetry approach to estimating littoral sediment transport include the atmospheric correction, spatial variability of depth within the sensor field-of-view, uncertainty in the bottom reflectance, variations in chlorophyll concentration, suspended sediment, bubbles, foam, and whitecaps.

Recent advances in the use of hyperspectral remote sensing and optimization procedures to derive shallow water depths have proven successful. Lee *et al*. (1998) developed a hyperspectral remote sensing reflectance model for shallow waters. The above-surface total remote sensing reflectance is used to determine the bottom albedo, absorption coefficients, and, ultimately, the bottom depth. For depths ranging from 2 to 20 m, the retrieved depth was accurate to within 5 percent (Lee *et al*., 1998). The radiative transfer (RT) numerical model, HYDROLIGHT (Mobley, 1995), was used by Lee *et al*. (1998) to determine different radiance distribution values for the specified water characteristics in their study.

The littoral sediment transport algorithm makes use of the VIIRS visible bands at 555 and 672 nm. Assuming that bottom relfectance does not change during sequential measurements, the algorithm retrieves bottom depth changes from remote sensing reflectance at 555nm. The bottom depth changes are directly related to LST values through a cell area and time elasped between two sequential measurements. The red band at 672 nm is used in accounting for possible changes to the water turbidity during the sequential measurements. Evaluation of the algorithm and sensitivity studies was done using simulated datasets. Simulations of remote sensing relfectance were carried out by using the HYDROLIGHT software. The simulations have shown that the algorithm is capable of meeting the SRD thresholds only for limited environmental conditions. By knowing the time elapsed between measurements, we can correlate the change in water depth to the change in bathymetry, which in turn is related to LST.

Global databases on properties of the littoral zone, to be developed before the implementation of the National Polar-orbiting Operational Environmental Satellite System (NPOESS) by high-resolution, hyperspectral sensors such as the Airborne Visible Infrared Imaging Spectrometer (AVIRIS), will provide first-guess information for algorithms using the moderate spectral/spatial resolution VIIRS observations. Also, the well-known phase and amplitude of depth variations driven by the tides can be exploited as a kind of “vicarious calibration signal” for fine-tuning bathymetry algorithms. Sediment transport events would be expected to have temporal and spatial scales clearly distinct from the tidal signals.

Littoral sediment transport is only required under clear/daytime conditions *[V-4].*

3.0 3.0 ALGORITHM DESCRIPTION

3.1 OVERVIEW AND BACKGROUND

Littoral sediment transport is defined as the change in the volume of sediment in the cell since the last measurement divided by the time interval between successive measurements: LST=$A\Delta h/\Delta t$, where A is the cell area, Δh is the bottom depth change, and Δt is the time interval. Therefore, LST retrieval is a bathymetry problem.

Passive remote sensing techniques for mapping shallow water depth and bottom features have been developed for more than 20 years (Lyzenga, 1978). The techniques were developed on the basis of simple seawater reflectance models using few spectral bands. A number of assumptions concerning bottom reflectivity and in-water diffuse light attenuation had to be accepted in developing the retrieval algorithms. Since that time considerable success has been achieved in developing both reflectance models and seawater inherent optical property (IOP) models. More recent algorithms are discussed in Philpot (1989) and Maritorena *et al*. (1994).

Past studies by Rosenshein, *et al.* (1977), Fryer *et al.* (1985), Tewinkel (1963), and Lyzenga (1981) have shown that it is possible to map bathymetry by using satellite and aircraft images. The different methods utilized included photointerpretation, photogrammetry, and computer analysis of multispectral satellite imagery. Photointerpretation is hindered by surface reflectance and by the fact that bottom color changes cannot be discerned readily from the ocean depth (Lyzenga, 1978). Thus, multispectral methods have advanced to the forefront of this field of research. Polcyn and Lyzenga (1973) and Weidmark *et al.* (1981) have shown the multispectral method to be successful when atmospheric effects, bottom reflectance, and water quality are invariant for the scene (Philpot, 1989). However, other studies have shown that it is difficult to determine accurately the reflectance and attenuation within the littoral region from satellite imagery. Cracknell *et al.* (1987) had little success in consistently extracting the ocean depth from multispectral imagery in regions where the water quality was highly variable.

Hyperspectral remote sensing has proven to be a promising tool for retrieving bottom depth and seawater IOPs from the remotely sensed reflectance of shallow waters (Lee *et al*., 1994; Lee *et al.*, 1998a and 1998b). One approach to simultaneously deriving depth and IOPs of shallow waters from hyperspectral measurements is analytical modeling. Analytical modeling is based on both reflectance models and IOP models. The shallow water reflectance model accounts for the contribution to the remotely sensed signal from bottom reflection and possible bottom fluorescence. The seawater IOP models parameterize in-water spectral absorption and backscattering as functions of seawater constituent concentrations. There are three major seawater constituents (or bio-optical parameters) that contribute to absorption and backscattering. They are phytoplankton pigments (mainly chlorophyll *a*), colored dissolved organic matter (CDOM), and suspended particulate matter (SPM). A whole model of the shallow seawater spectral reflectance contains a set of unknowns: bottom depth, bottom reflectivity, and seawater bio-optical parameters. The unknowns are derived from minimization of the spectral difference between the modeled and measured reflectance.

It is well known that the Navy is currently in the process of shifting away from open ocean warfare to joint littoral warfare. In order to support that effort, the Navy and Marine Corps will need more detailed information about the shallow waters of the littoral region, such as

bathymetry, visibility, bottom type, and water clarity, and consequently, information to assist in the detection of underwater hazards, mines, and submarines.

Present day instruments have resolutions that are too large (1 km) to adequately obtain information within the very complex littoral zone. Other instruments with a sufficient resolution do not have the correct bands to penetrate the waters and have unacceptable SNR. Landsat and SeaWiFS do not have sufficient spectral bands to resolve the spectral signatures within this region (Wilson, 1998). Thus, "the ideal coastal ocean instrument would have high spectral resolution and high signal to noise for maximum water penetration and moderate spatial resolution for resolving the complexities of the coastal ocean" (Davis, 1997). Such an instrument, which is being developed under the direction of the Office of Naval Research, is the Coastal Ocean Imaging Spectrometer (COIS)

Hyperspectral sensors use tens to hundreds of bands to collect and record data. A main difference between multi-spectral and hyperspectral sensors is the fact that hyperspectral sensors use more bands that are 10 nm wide contiguous spectral bands. By increasing the number of bands implemented, subtler changes in the spectral signature can be detected which are otherwise missed in multispectral imagery.

As stated above, present day instruments have a resolution that is too large (1 km) to adequately obtain information within the littoral zone. It is particularly difficult to collect data pertaining to the main use of the littoral sediment transport product, which is mine detection operations and design of mine warfare systems.

This is the general context for analytical algorithms for the simultaneous retrieval of bathymetric and bio-optical parameters from remotely sensed hyperspectral reflectance. There are several examples of the application of analytical algorithms for retrieving the bio-optical parameters of seawater. They can be found, among other places, in the work of Lee *et al.* (1994) Roesler and Perry (1995), Hoge and Lyon (1996), Garver and Siegel (1997), and Vasilkov (1997).

The algorithm described in this document is intended to derive bottom depth changes, Δh, from two successive measurements of water-leaving radiances at two wavelengths: 555 and 672 nm. It is assumed that bio-optical properties of seawater may vary between two successive measurements.

3.2 PROCESSING OUTLINE

Figure 1 presents a schematic flowchart for the littoral sediment transport algorithm. VIIRS wavelengths, 555 and 672nm, are utilized to determine the retrieval depths, which in turn, are used to compute the littoral sediment transport.

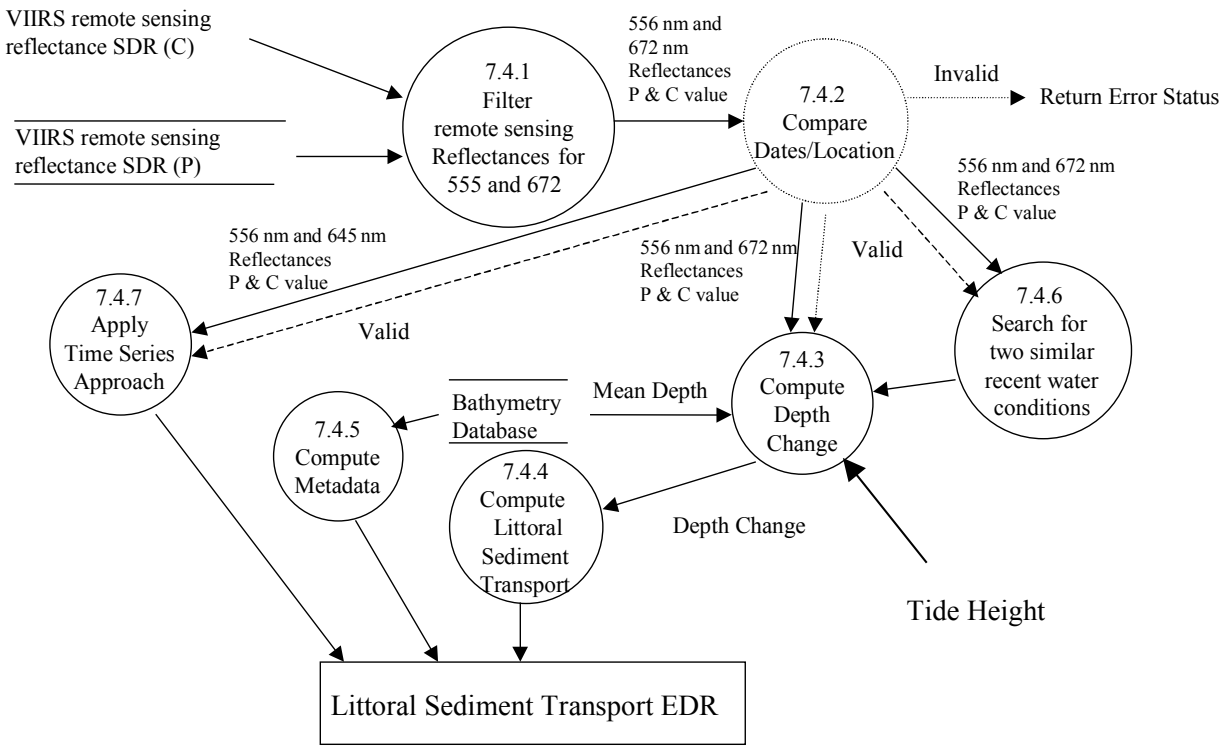

VIIRS Littoral Sediment Transport EDR Level 2 Data Flow Diagram

Figure 1. Schematic flowchart of the littoral sediment transport algorithm.

3.3 ALGORITHM INPUT

3.3.1 VIIRS Data

Remote sensing reflectance in two VIIRS visible bands (555 and 672 nm) is required as inputs for the LST retrieval algorithm. The remote sensing reflectance values are the outputs of an atmospheric correction algorithm. Because the visible bands are being used as input to this EDR the same masks and flags are used as are used for the ocean color data. Please see the Ocean Color ATBD for descriptions of the masks and flags used to produce the LST EDR.

3.3.2 Non-VIIRS Data

Non-VIIRS data sets are needed for an atmospheric correction algorithm only. They include total ozone amount, atmospheric pressure, surface wind velocity, and precipitable water.

3.4 THEORETICAL DESCRIPTION OF LITTORAL SEDIMENT TRANSPORT RETRIEVALS

3.4.1 Physics of the Problem: Radiance and Seawater Optical Properties Models

Let us denote reflectances at 555 and 672 nm as R_4=R(555), R_5=R(672). The remote sensing reflectance, R_{rs}, is expressed through the diffuse reflectance, R, by Equation (2) given below. The main assumptions of the algorithm are:

1. Bottom albedo is not changed during two successive measurements made for the retrieval of littoral sediment transport.

2. Bottom albedo does not affect the red band reflectance, R_5. This means that $[K_d(672)+K_u(672)]h>>1$, where K_d and K_u are the diffuse attenuation coefficients for downwelling and upwelling radiation respectively, and h is the bottom depth.

3. Changes of chlorophyll and dissolved organic matter (DOM) absorption are negligible at wavelengths 555 and 672 nm. This means that the suspended particulate matter is a major seawater constituent whose variation determines the optical properties of seawater, and hence the seawater reflectance and diffuse attenuation of in-water radiation.

4. Bottom albedo is much greater than the deep seawater diffuse reflectance, R_∞, at wavelengths of 555 and 672 nm. This is valid for sandy bottoms, where reflectivity is approximately 20 percent (Lyzenga, 1978).

5. Bottom slope is sufficiently small.

Seawater is usually more transparent at 488 nm than at 555 nm except for DOM absorption dominant coastal waters and highly productive waters. However, using of the 488 nm band instead of the 555 nm band may not be recommended for the LST retrieval. Chlorophyll and DOM absorption significantly affects the seawater reflectance at 488 nm. Therefore, changes of chlorophyll and DOM can result in variations of the reflectance exceeding the effects of bottom depth changes on the reflectance. This occurs because of exponential decay of the bottom reflectance contribution to the seawater reflectance. Independent retrievals of chlorophyll and DOM absorption are necessary to account for their effects on the reflectance at 488 nm. The VIIRS chlorophyll algorithm works only for deep waters not affected by bottom reflectance.

A basic equation comes from Philpot (1989) and Maritorena *et al.* (1994):

$$R=R_\infty [1 - \exp(-\alpha h)] + R_b \exp(-\alpha h) \quad (1)$$

where α is the effective attenuation coefficient. Dependence on wavelength is omitted in Equation 1. Remote-sensing reflectance is proportional to the reflectance (Gordon *et al.,* 1988):

$$R_{rs} = \frac{t_1 t_2}{Q n^2} \frac{R}{1 - \gamma R} \quad (2)$$

where t_1 and t_2 are transmittance of the sea surface for downwelling irradiance and upwelling radiance, n is the refractive index of seawater, and γ=0.48 is the water-to-air internal reflection coefficient. The water-to-air radiance divergence factor is $t_1 t_2/n^2$ =0.518 (Lee *et al.,* 1998).

There are three unknown functions of wavelength in Equation 1. They are the deep water reflectance, R_∞, the bottom albedo, R_b, and the effective attenuation coefficient, α. Given the only known function—the measured spectral reflectance—a number of assumptions are made to derive the water depth from Equation. 1.

The first and simplest assumption is the invariability of all three functions over the scene (Lyzenga, 1978 and Philpot, 1989; *see also* a comprehensive list of references in the latter paper). Then, the deep-water reflectance is determined from measurements over optically deep

pixels. However, for LST retrieval purposes the assumption of invariable attenuation coefficient may not be valid. Therefore, even the deep-water reflectance is unknown in this case.

According to the second assumption, the deep water reflectance at 672 nm is simply the measured reflectance: $R_{\infty 5} = R_5$. The deep-water reflectance at 555 nm can be determined from a model of seawater reflectance.

Many approaches exist to obtain an approximate solution to the radiative transfer equation, which can serve as the marine reflectance model (Gordon, 1973; Golubitskiy and Levin, 1980; Zaneveld, 1982; Aas, 1987; Haltrin and Kattawar, 1993). They are based on two main physical properties of seawater: 1) Scattering is highly anisotropic in the forward direction; and 2) seawater is an absorbing medium. They give roughly similar dependence of the reflectance on the IOP: the seawater absorption coefficient, a, and the seawater backscattering coefficient, b_b. The simplest version of this dependence (Morel and Prieur, 1977) can be expressed as:

$$R\infty(\lambda) = const \frac{b_b(\lambda)}{a(\lambda)} \tag{3}$$

According to the third assumption, the absorption coefficient in this equation is equal to the pure seawater absorption coefficient, a_w. Note that $a_w(555)=0.067$ m^{-1} and $a_w(672)=0.42$ m^{-1}. Neglecting the Rayleigh scattering and assuming wavelength-independent SPM scattering, we arrive at the deep-water reflectance at 555 nm as proportional to the seawater diffuse reflectance at 672 nm:

$$R_{\infty 4} = S_1 R_{\infty 5}$$

where $S_1 = a_w(672) / a_w(555)$. A more precise value of this proportionality coefficient can be determined from simulations using, for example, HYDROLIGHT software (Mobley, 1995).

The diffuse attenuation coefficient is proportional to the sum of the absorption coefficient and the backscattering coefficient. Hence, $\alpha = 2 f (a + b_b)$, where f is a geometrical factor. To account for the effect of SPM variation on the diffuse attenuation coefficient at 555 nm, we express the attenuation coefficient through the reflectance using Equation 3:

$$\alpha = 2 fa(1 + const R_\infty)$$

From this expression we obtain:

$$\alpha_4 = 2f[a_w(555) + a_w(672)\, R_5\, S_2\,]$$

where S_2 is an unknown coefficient to be determined from exact simulations. According to a fourth assumption, Equation 1 can be rewritten in a form similar to Lyzenga's (1978):

$$R - R_\infty = R_b \exp(-\alpha h) \tag{4}$$

Thus, Equation 4 can be written for wavelength 555 nm as follows:

$$\ln (R_4 - S_1 R_5) = \ln R_b - 2f[a_w(555)+a_w(672) R_5 S_2] h \quad (5)$$

Consequently, for small bottom depth changes we obtain, taking into account the first assumption:

$$(\Delta R_4 - S_1 \Delta R_5)/(R_4 - S_1 R_5) = -2 f[a_w(555)+a_w(672) R_5 S_2] \Delta h - 2f a_w(672) S_2 h \Delta R_5 \quad (6)$$

In this relationship, quantities R_4 and R_5 may be taken as an average of two successive measurements, and the value of h may be taken from bathymetry data sets. It is interesting that the bottom depth change does not depend on the bottom albedo. The final expression for Δh is

$$\Delta h = \frac{\frac{S_1 \Delta R_5 - \Delta R_4}{R_4 - S_1 R_5} - 2 f a_w(645) S_2 \Delta R_5 h}{2 f [a_w(556) + a_w(645) R_5 S_2]} \quad (7)$$

Simulations using HYDROLIGHT verified this expression. The simulations also gave precise values of parameters f, S_1, and S_2.

Alternative approaches:

A. Time Series Approach

Applying a time series approach may reduce considerably the littoral sediment transport retrieval errors. The approach is promising, if the customer is interested mainly in littoral sediment transport tendency and real-time data is not a high priority. In such a case, individually retrieved values of the littoral sediment transport EDR are stored as a time series for further processing. Littoral sediment transport values available at the moment are fitted by a polynomial function of time. A least-squares technique will be used for best fitting. An order of the polynomial may be adjusted as new data becomes available.

Using HYDROLIGHT simulations for two types of bottom depth changes tested the time series approach: a linear decrease and an abrupt increase in the bottom depth that models a storm event. A major goal of the simulations was to test the capability of the littoral sediment transport algorithm to monitor the littoral sediment transport tendency. In the first case, the bottom depth was assumed to be a linear function of the simulation number: $h = h_0 - k (n-1)$, i.e. true values of the bottom depth change are $\Delta h = - k (n-1)$, n=1,N. In the second case, the bottom depth is a step function of the simulation number, i.e. true values of the bottom depth change are $\Delta h = 0$, if n <= N/2 and $\Delta h = \Delta h_0$,if n > N/2.

Figures 2 and 3 display the results from the time series analyses for the case of linear change of the water depth. Remote sensing reflectances at 555 and 672 nm were calculated by using the HYDROLIGHT software. To model effects of sensor radiometric noise on LST retrievals, the remote sensing reflectances were perturbed using a random number generator. Only a single sample of random numbers was applied to the time series of the remote sensing reflectance. The standard deviation of perturbations in both bands was equal to 5%. The results show that LST retrievals for low chlorophyll concentrations meet the accuracy threshold of 30% for unperturbed reflectances. Perturbations considerably affect the retrievals only in the range of depth changes up to 2 m. The LST retrievals for high chlorophyll concentrations meet the accuracy threshold

only for big depth changes exceeding about 3 m. In the range of depth changes up to 3m the perturbations dramatically affect the retrievals. The effects of the radiometric noise on LST retrievals will be studied in more detail in the future.

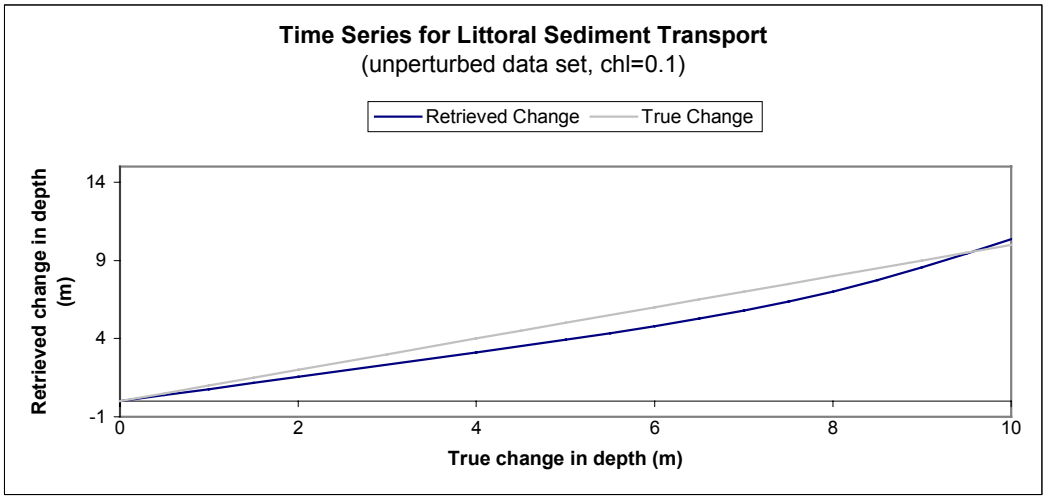

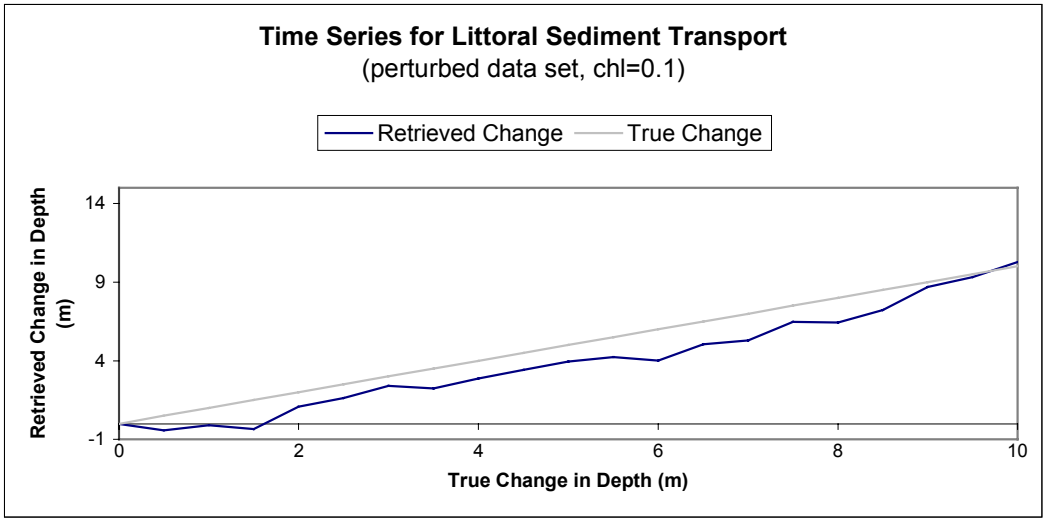

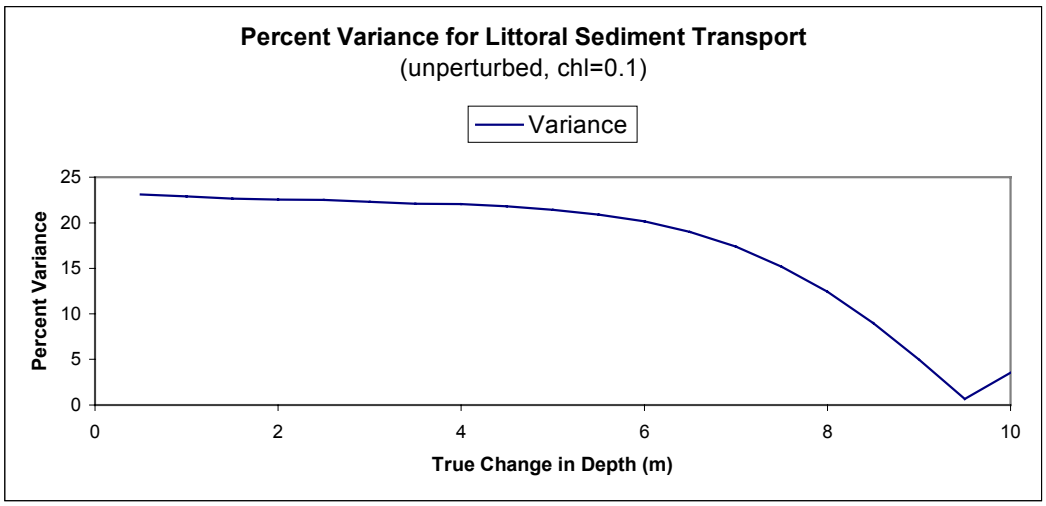

Figure 2. Time series analysis for LST for a chlorophyll concentration of 0.1 mg/m^3.

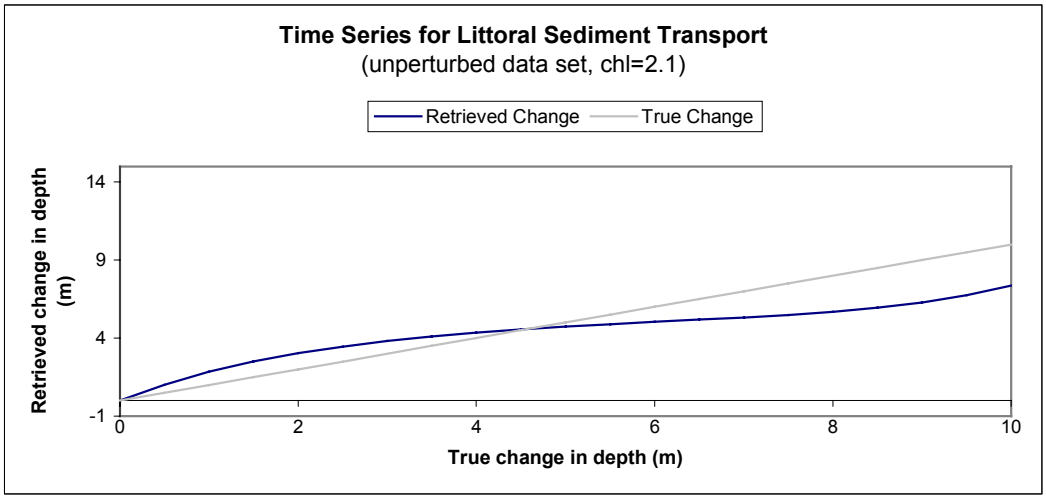

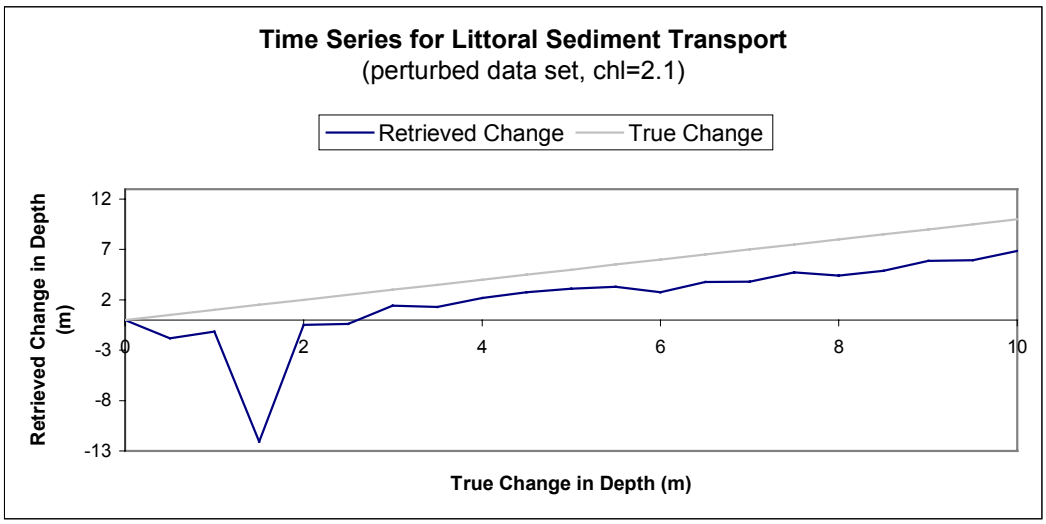

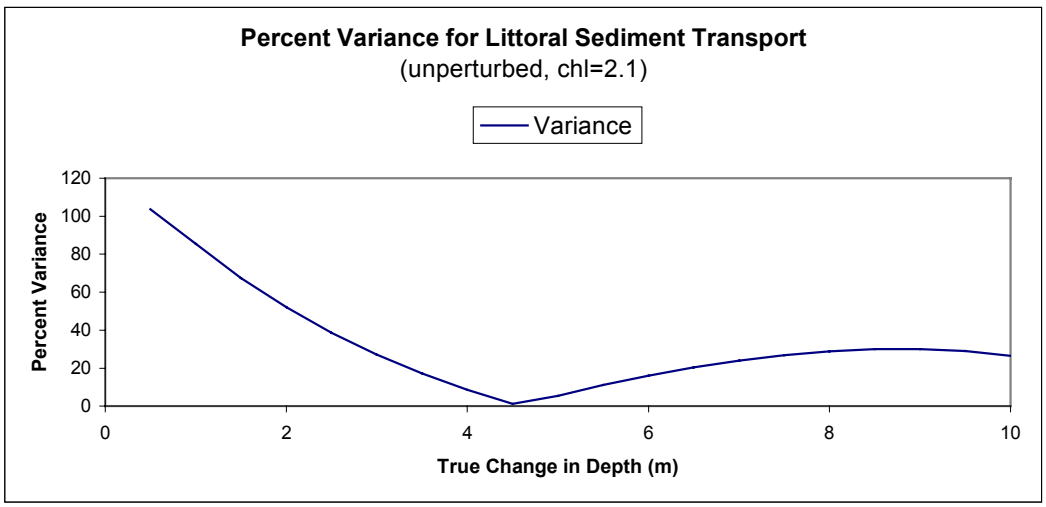

Figure 3. Time series analysis for LST for a chlorophyll concentration of 2.1 mg/m^3.

B) Band Ratio of R(412)/R(672) to Account for Absorption Changes

Absorption changes in the band at 555 nm may affect strongly the retrievals of littoral sediment transport because the littoral sediment transport algorithm uses the assumption that the absorption at this band is constant. According to simulation results presented in Fig. 4, chlorophyll changes of about 2 mg/m^3 are equivalent to bottom depth changes of approximately 1.5 m. Thus, any littoral sediment transport algorithm using this band would not be able to distinguish between chlorophyll changes and bottom depth changes, if there is no available absorption information for this band. The reflectance ratio of R(412)/R(672) can account for possible absorption changes. As a consequence of this approach, the littoral sediment transport algorithm assumption that states that chlorophyll and DOM absorption are negligible at 555 nm can be removed.

According to this approach, it is assumed that the absorption coefficient of water constituents at 555 nm is expressed through a regression relationship:

$$a_{const} = A\frac{R(645)}{R(412)} + B$$

where A and B are the regression coefficients to be determined. Then, the expression for the parameter, S1, can be written as:

$$S_1 = \frac{a_w(645)}{a_w(556) + AR(645)/R(412) + B}$$

The regression coefficient can be derived from HYDROLIGHT simulations for variety of seawater optical properties.

Results will be presented in future ATBDs.

C) Red Band Shift to 672 nm

The shift of the red band to 672 nm benefits greatly the littoral sediment transport algorithm. Therefore, the basic assumption that there is no bottom reflectance effect on the red band reflectance becomes readily more acceptable. Therefore, the algorithm willwork for smaller bottom depths.

D) Flag parameter

The littoral sediment transport estimates from VIIRS could be used as a flag for areas with possible bottom changes. Once the data is flagged, an instrument with a higher spatial resolution and most likely a greater number of spectral bands then could view the region. Possible instruments for this type of follow-on would be Landsat, AVIRIS, and other hyperspectrally equipped aircraft. Essentially, a large footprint sensor, such as VIIRS, would be used to obtain optical properties and characteristic statistics for the world oceans. Over time a historic database of the bottom depths and optical properties would be recorded. From this, changes in the bathymetry could be detected and compared to the database. If a flag is obtained detecting that a

drastic change in depth has occurred in a region, then more information could be gathered for the region by sending in a high-resolution instrument, such asAVIRIS. The NPOESS/VIIRS could be used as an indicator as to when to send in the hyperspectral instruments for further study.

3.4.2 Verification of Basic Assumptions

Exact simulations using the HYDROLIGHT software verified some assumptions of the algorithm. Below are results for an IOP model of Case 1 waters. The only basic assumption to be verified is the third assumption, i.e., that chlorophyll absorption is negligible at a wavelength of 555 nm. Other assumptions are always valid or can be valid for specific values of bottom depth and bottom albedo.

Simulated seawater reflectance at wavelength 555 nm is shown in Figure 4 as a function of bottom depth for different chlorophyll concentrations. The bottom albedo is 20 percent. The DOM absorption is fully correlated to chlorophyll absorption for Case 1 waters, so it is not considered separately. It can be seen from Figure 4 that the fourth assumption is not strictly valid. For example, at a water depth of 6 m, the reflectance decreases about 18 percent when chlorophyll concentration increases by a factor of about 20 (from 0.1 mg/m^3 to 2.1 mg/m^3). This reflectance decrease seems to be small when taking into account the large range of chlorophyll changes, but it is equivalent to bottom depth change from 6 m to about 7.7 m. That means that the third assumption may contribute significantly to the algorithm error budget. It should be noted that the effect of chlorophyll changes is much more pronounced for the VIIRS band at 488 nm. That is why this band is not used in the LST algorithm.

A rough estimate of the parameters S_1, the ratio of deep water reflectance at 555 nm to that at 672 nm, is the ratio of pure water absorption coefficients: $a_w(672)$ / $a_w(555)$. HYDROLIGHT simulations verified this estimate. Comparison of this estimate with exact calculations is shown in Figure 5 for different chlorophyll concentrations. It is clear from Figure 5 that the estimate of S_1 in the form of the seawater absorption coefficient ratio is quite good.

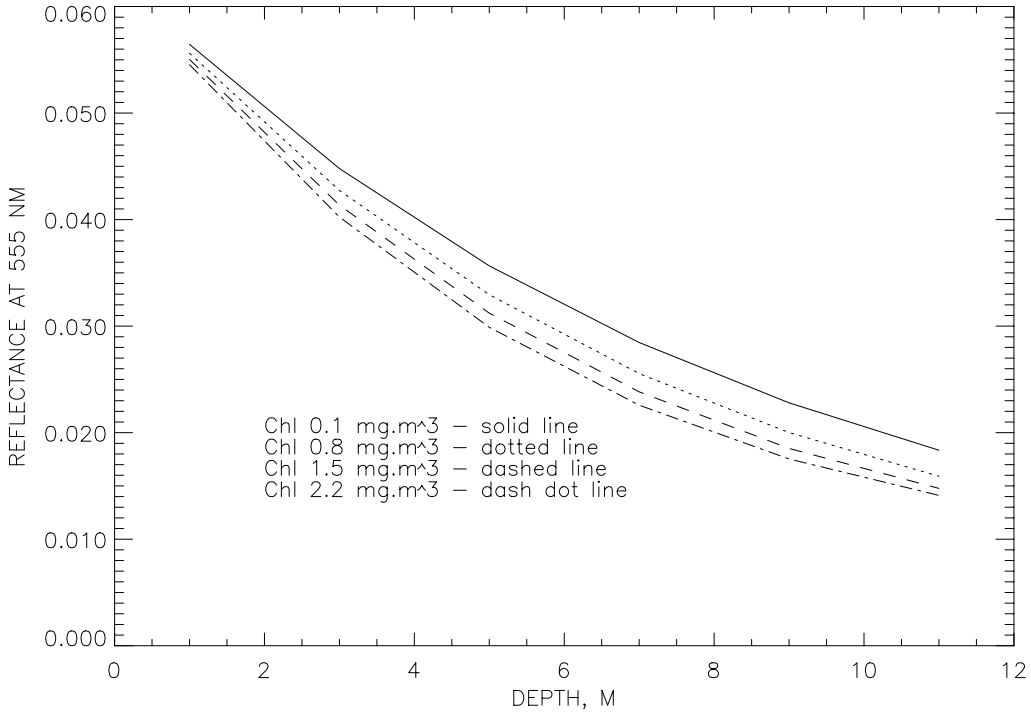

Figure 4. Seawater reflectance as function of water depth.

To reduce the error budget in the LST algorithm, it is necessary to account for chlorophyll variance between two successive measurements. Additional assumptions are needed to obtain an estimate of chlorophyll concentration. The VIIRS estimate of chlorophyll may not be reliable for the same pixel that the LST is estimated because of the bottom reflectivity effects. If the horizontal distribution of chlorophyll is assumed to be homogeneous, then the adjacent pixels for deep water can be used to estimate the chlorophyll variance.

It is also reasonable to assume that the chlorophyll concentration does not vary considerably during two successive measurements, even though the SPM concentration varies significantly. Generally, coastal waters are Case 2 waters in which bio-optical properties of seawater are not correlated. Storms considerably change the SPM concentration because of immediate bottom resuspension. However, the chlorophyll concentration may remain invariable because its change results from biological processes that have a characteristic time response of about a day and/or biogenic element concentration that remain constant. Because the chlorophyll concentration is invariable, the algorithm accounts for possible variance in SPM concentration during two successive measurements.

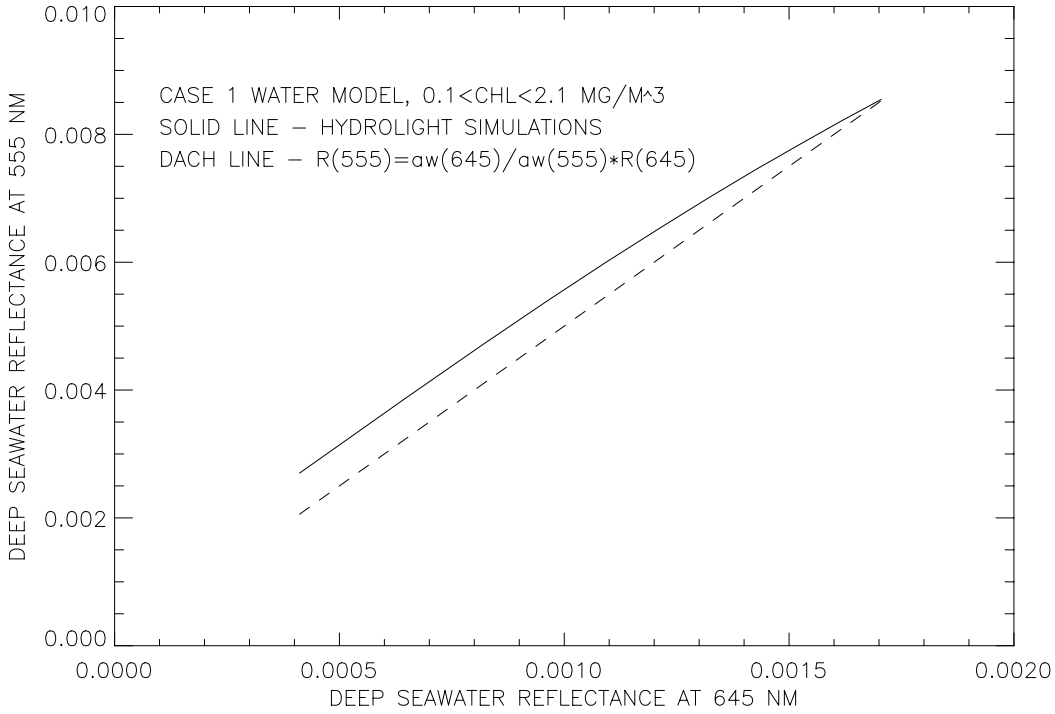

Figure 5. Deep sea-water reflectance at 555 nm versus reflectance at 672 nm.

3.4.3 Archived Algorithm Output

The only archived algorithm output for the littoral sediment transport EDR are values of depth and transport.

3.4.4 Variance and Uncertainty Estimates

Further research is required to ascertain the variance and uncertainty of the littoral sediment transport algorithm.

3.4.4.1 Error Budget

Sensor calibration and stability error, sensor radiometric noise, atmospheric correction algorithm error, tidal height error, and the littoral sediment transport algorithm error are the main components of the error budget. Preliminary results displayed in section 3.4.2 show estimates of the algorithm error. Currently, it appears that it is the littoral sediment transport algorithm itself that contributes the most to the error budget. Table 1 displays the error budget for the littoral sediment transport EDR.

Detailed Basis for Error Allocations

There are two major sources to the Littoral Sediment Transport (LST) algorithm errors. The first major source is the remote sensing reflectance and the second is the retrieving algorithm. The remote sensing reflectance (or water-leaving radiance) is the output from the atmospheric

correction algorithm. Both the atmospheric correction algorithm and sensor cause remote sensing reflectance errors. An analysis of the remote sensing reflectance errors is done separately.
The retrieving algorithm error is of two types: random and systematic. The temporal and spatial variability of the bottom reflectivity largely causes the random error. The systematic error is due to the bottom slope and approximate reflectance model used in the LST algorithm. The LST algorithm assumes a flat bottom, therefore, natural bottom slopes cause an error that can be considered as a systematic error.

Time Series Approach

Applying a time series approach may reduce considerably the littoral sediment transport retrieval errors. The approach is promising, if the customer is interested mainly in littoral sediment transport tendency and real-time data is not a high priority. In such a case, individually retrieved values of the littoral sediment transport EDR are stored as a time series for further processing.

Remote sensing reflectance errors

The remote sensing reflectance error was estimated by averaging the retrievals over the geometrical conditions of a satellite orbit. It was assumed that the SZA range was between 0 to 70 degrees, and the viewing zenith angle range was between 0 to 46 degrees. Both the accuracy and precision of the remote sensing reflectance were calculated. Pixel aggregation was not performed because of the LST horizontal cell size threshold of 1.3 km.

To simulate the effects of the remote sensing reflectance on the LST retrievals, the following procedure was adopted. The remote sensing reflectance was calculated for given depths by using the Hydrolight software (Mobley, 1995). True values of the remote sensing reflectance at 555 and 670 nm were perturbed by systematic and random errors. Values of the systematic error in every spectral band were determined by the accuracy of the remote sensing reflectance provided by the atmospheric correction algorithm. The random error was assumed to be gaussian. The standard deviation of the random error was determined by the precision of the remote sensing reflectance. Approximately 500 samples of the random error were generated for the given bottom depth. Bottom depth changes were retrieved from the noisy reflectance spectra by using the Vasilkov algorithm (Mullen and Vasilkov, 1999). The LST accuracy and precision were calculated from the retrieved values of the bottom depth change.

Two models of the seawater inherent optical properties (IOP) were used in the Hydrolight simulations. The first one was the Case 1 water model (Morel, 1988). According to this model, the chlorophyll concentration is the only input parameter of the IOPs. For Case 2 waters, a reflectance model based on empirical regressions (Tassan, 1994) was used (Vasilkov, 1997). According to this model, the seawater backscatter is higher for a given chlorophyll concentration than for the Case 1 model.

The reflectance errors used in the calculations of their effects on the SPM retrievals correspond to the following conditions: the baseline VIIRS model radiometric noise, spectrally-correlated calibration error of 0.5%, and whitecap reflectance error related to a wind speed of 6 m/s with an uncertainty of 1 m/s.

Bathymetry

The LST algorithm uses bathymetry as ancillary data to retrieve the LST EDR. Uncertainties in the bathymetric data play a minor role in the LST error budget. For example, if seawater optical properties do not change between two successive measurements, the bathymetric data will not affect the LST retrievals at all; i.e. any uncertainty in the bathymetric data is acceptable. The effect of the bathymetric data uncertainty on the LST retrievals was estimated analytically. Roughly, the LST relative error is proportional to the bathymetric relative uncertainty multiplied by the relative change of the red band reflectance caused by the change of the seawater optical properties. Assuming the bathymetric data uncertainty is approximately 20% and the red band reflectance change is approximately 20%, then the LST error will be less than 5%.

Tides

Tide heights are calculated for every location and time by using hydrodynamic models along with information about bottom topography. An example of the comparison of the modeled and observed tide heights is shown in Figure 6. Data on Figure 6 was obtained from the Web site tidesonline.nos.noaa.gov. It is seen that errors of the tide height prediction from the models may be as large as 0.1 m. This tide height error is not negligible in comparison with possible LST values, therefore, it should be accounted for in the error budgets.

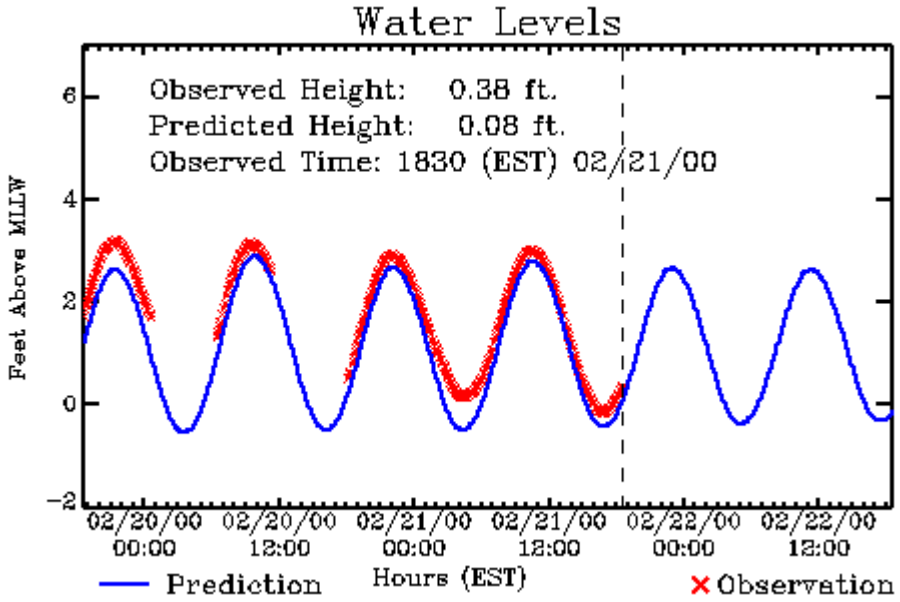

Figure 6. Comparison model-predicted tide heights with observed ones.

LST Algorithm Errors

The LST algorithm assumes both, spatially and timely, invariable bottom reflectivity and a flat bottom. The time and spatial variability of the bottom reflectivity and bottom depth variability within the horizontal cell will contribute to the random algorithm error. To estimate this error, MODIS Airborne Simulator (MAS) data obtained over shallow waters was used. MAS pixels

were aggregated up to the cell size of 1.3 km. Spatial variations of atmospheric properties across the cell were not assumed. Standard deviations of TOA reflectances were calculated at 555 and 670 nm. The variability in the reflectance at 670 nm is caused only by the spatial inhomogeneity of water turbidity, while bottom reflectivity, bottom depth, and water turbidity inhomogeneities cause the variability in the reflectance at 555 nm. Subtracting the standard deviation at 670 nm from the standard deviation at 555 nm, we can estimate the reflectance error due to the variability of the bottom reflectivity and bottom depth across the horizontal cell. A corresponding error in the LST is estimated from the basic equation of the LST algorithm

$$R=R_\infty [1 - \exp(-\alpha h)] + R_b \exp(-\alpha h)8$$

where R is the shallow water the reflectance, R_∞ is the deep water reflectance, R_b is the bottom reflectance, α is the effective attenuation coefficient, and h is the bottom depth. If ΔR is the reflectance error, the corresponding error in the bottom depth will be

$$\frac{\Delta h}{h} \approx \frac{\Delta R}{R_\infty + R_b} \frac{\exp(\alpha h)}{\alpha h} \qquad (9)$$

The reflectance error estimated from MAS data collected over shallow waters is about 0.001. Assuming the bottom reflectance is approximately 0.1 and the value of αh does not exceed 3, we obtain an estimate of $\Delta h/h \approx 0.08$.

The LST algorithm systematic error caused by the approximate reflectance model was estimated by the comparison of the LST retrievals from the remote sensing reflectances calculated by Hydrolight with the true LST values. The systematic error depends on the water type and chlorophyll concentration.

An estimate of the algorithm error caused by the bottom slope can be determined by assuming a linear dependence of the bottom depth on the horizontal distance, x: $h = h_0 + kx$, where h_0 is the bottom depth at the horizontal cell center. Integrating equation (1) over the horizontal cell size L and expanding hyperbolic sinus in a series on the small parameter $(\alpha kL) / 2$, we obtain the reflectance error

$$\Delta R = (R_b - R_\infty) (\alpha k L)^2 / 12.$$

+This reflectance error should be substituted into equation (9) in order to obtain an estimate for the LST error. Assuming that $\alpha = 0.2$ m^{-1}, $h = 15$ m, $L = 1$ km, and allocating the LST error to be 15% for this error source, we obtain that the bottom slope should not exceed a value approximately $k = 0.25\%$.

Other sources of error for an optical bathymetry approach to estimating littoral sediment transport are sensor variability of depth within the sensor field of view, uncertainty in bottom reflectance, variations in chlorophyll concentration, and suspended sediments. However, further studies are needed to adequately determine the error budget.

3.5 ALGORITHM EVALUATION AND SENSITIVITY STUDIES

3.5.1 Algorithm Evaluation

Evaluation of algorithm performance was conducted using simulated data sets obtained using the HYDROLIGHT software. Most simulations were done for a Case 1 water reflectance model (Morel, 1988). Chlorophyll concentration is the only input bio-optical parameter of this model. The simulations were carried out for different chlorophyll concentrations and different water depths. Vertical distribution of the chlorophyll concentration was accepted as uniform. Other environmental parameters were taken to be constant. They are a solar zenith angle of 20^0, a bottom albedo of 20 percent, and a wind speed of 5 m/s. The bottom depth change was one meter in all simulations.

Let us consider first the evaluation results for the case of invariable optical properties of seawater, i.e., for invariable chlorophyll concentration. The accuracy of predicting the bottom depth change by the LST algorithm is shown in Figure 7 as a function of chlorophyll concentration for three initial depths. A measurement accuracy threshold of 30 percent *[V-31]* is shown as solid horizontal lines. Algorithm parameter values used are f=1.1 (Lee et al., 1994), $S_1 = a_w(672) / a_w(555)$, and S_2 =16. The S_2 parameter value was accepted from the comparison of the LST accuracy results for different values of this parameter. The value accepted may not be optimal because of the possible lack of the appropriate number of simulation runs. The algorithm accuracy meets the accuracy threshold within the chlorophyll concentration range of 0.4 – 2.0 mg/m^3. This range is expected in clear coastal waters for which the Case 1 water reflectance model is appropriate.

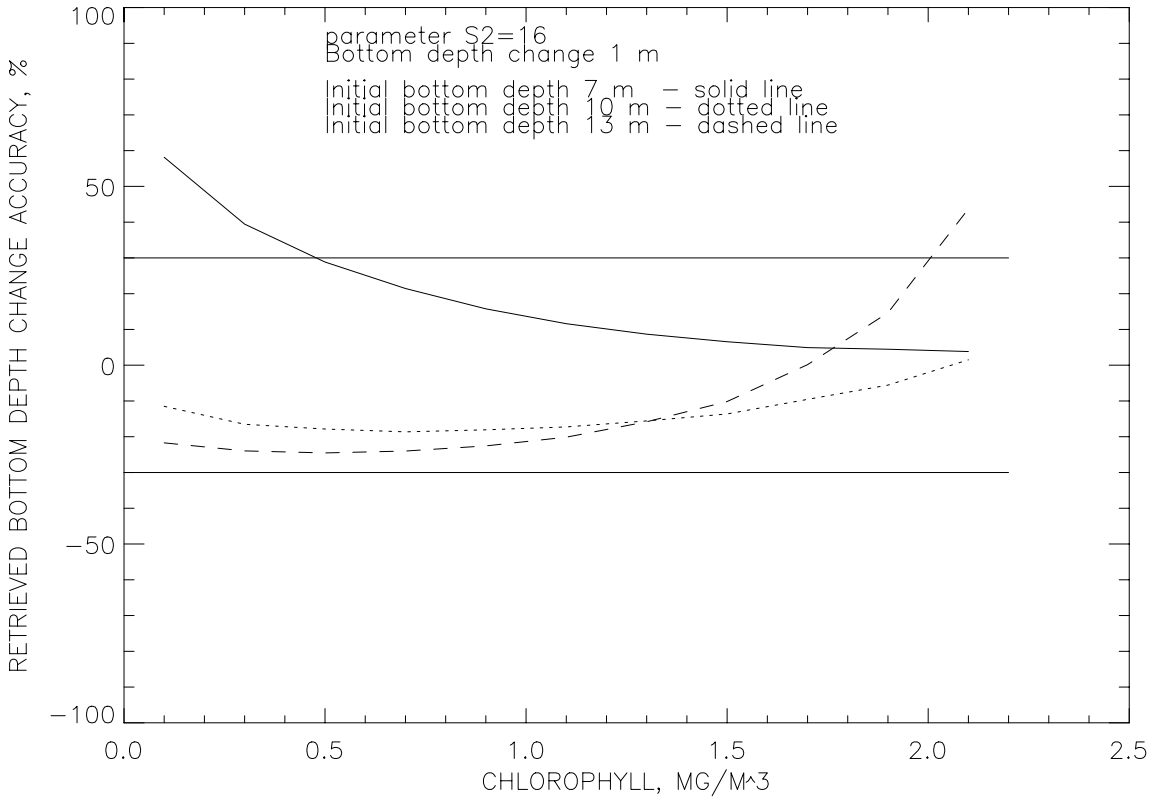

Figure 7. Accuracy of bottom depth change retrievals as a function of chlorophyll concentration assumed to be invariable.

The algorithm retrieval becomes less accurate as chlorophyll is allowed to vary between two successive measurements. Figure 8 shows algorithm accuracy as a function of initial chlorophyll concentration for different final chlorophyll concentrations. The initial depth is 10 meters. Figure 8 shows that the algorithm accuracy meets the accuracy threshold if chlorophyll concentration changes within a range of 0.7 – 1.7 mg/m^3.

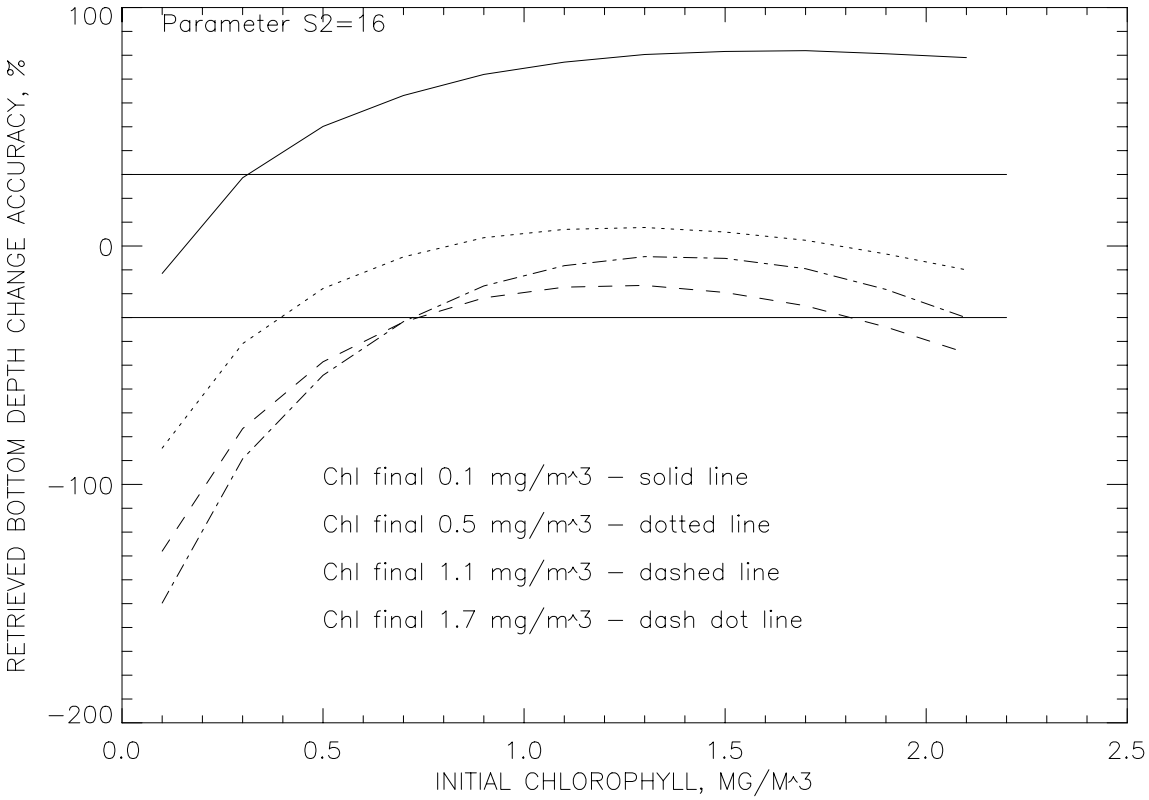

Figure 8. Accuracy of bottom depth change retrievals as a function of initial chlorophyll concentration.

Initial evaluation of the algorithm performance was made for the optical property model of Case 1 waters. However, coastal waters are Case 2 waters. Thus, simulations for an optical property model of Case 2 waters are in progress.

The algorithm performance may be improved by using an independent estimation of chlorophyll concentration and DOM absorption obtained from VIIRS chlorophyll products. Unfortunately, making use of this estimation is not straightforward. This is difficult because of the necessity of making additional assumptions pertaining to the spatial distribution of seawater optical properties and effects of the sea bottom reflectivity on the estimation. This issue will be addressed in future studies.

The mapping uncertainty has posed a problem for this EDR. The spatial scales for littoral sediment transport are on the order of tens of meters. Therefore, a spatial resolution of 30 m is desirable. However, the current sensor design has a 1.3 km resolution. Fortunately, a secondary application of the littoral sediment transport product is sandbar location and migration. These are on the scales of hundreds of meters. Thus, the 1.3 km resolution could be utilized only to give a rough estimate of migration (Figure 9). Figure 10 shows that the mapping uncertainty is a difficult criterion to meet with the 1.3 km spatial resolution. The uncertainty depends greatly on the bottom slope. The sloping bottom is a major problem for low spatial resolution sensors.

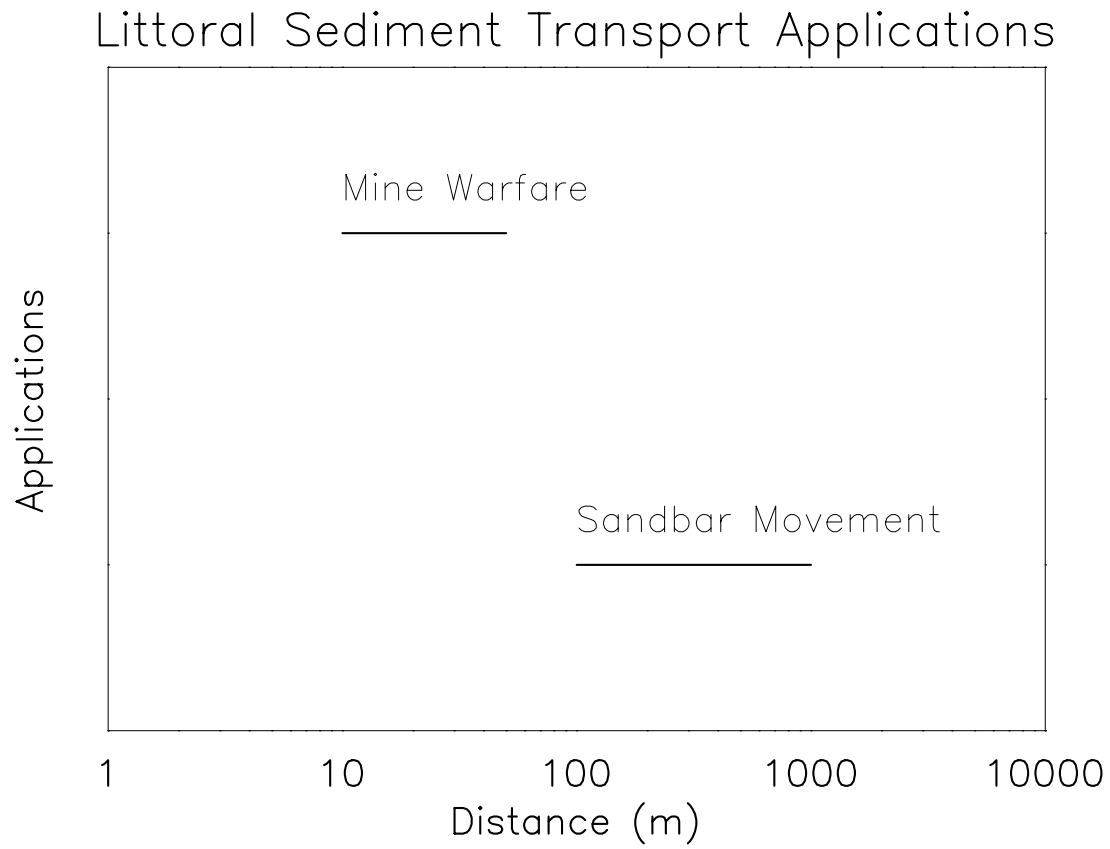

Figure 9. Littoral sediment transport applications.

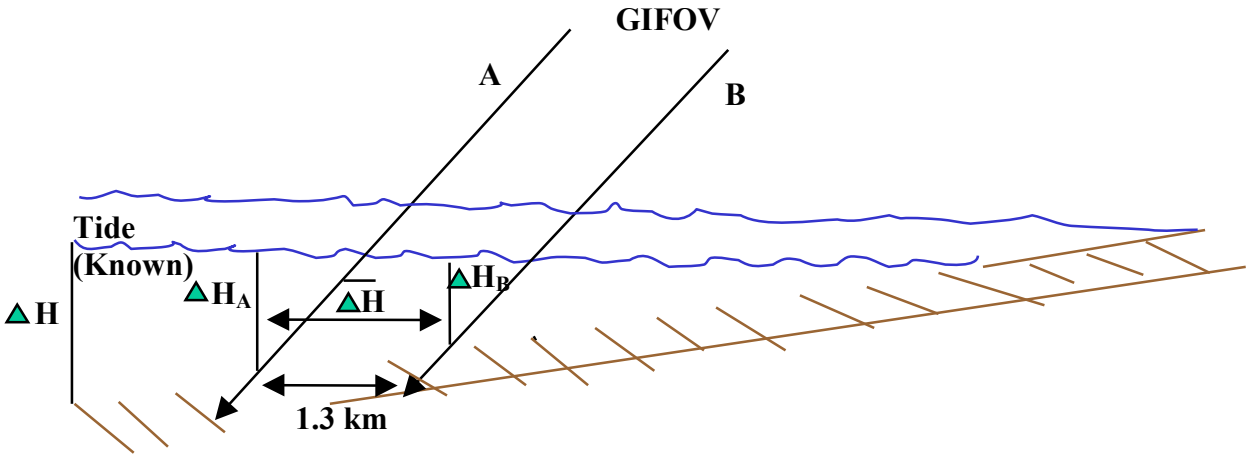

Figure 10. Mapping uncertainty, 5% slope, 0.5 m precision, and 1.3 km resolution.

Figures 11 and 12 show the effects on the retrieved depth error when the mapping uncertainty increases. The cells are shifted to deeper waters from starting depths ranging from 2 – 10 m. The algorithm results are especially poor in shallow waters because the assumption pertaining to the red band is not valid. It is assumed that the reflectance in the red band does not depend on depth.

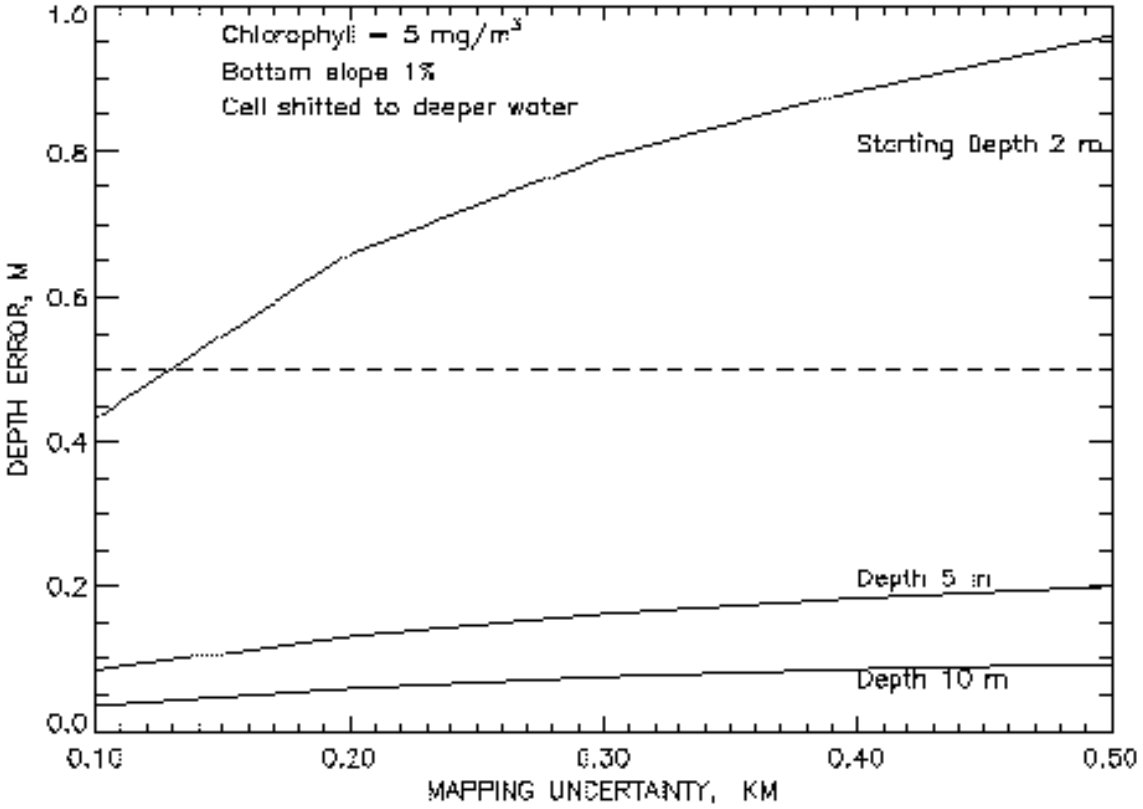

Figure 11. Mapping uncertainty and depth error for a chlorophyll value of 5 mg/m^3 with different starting depths.

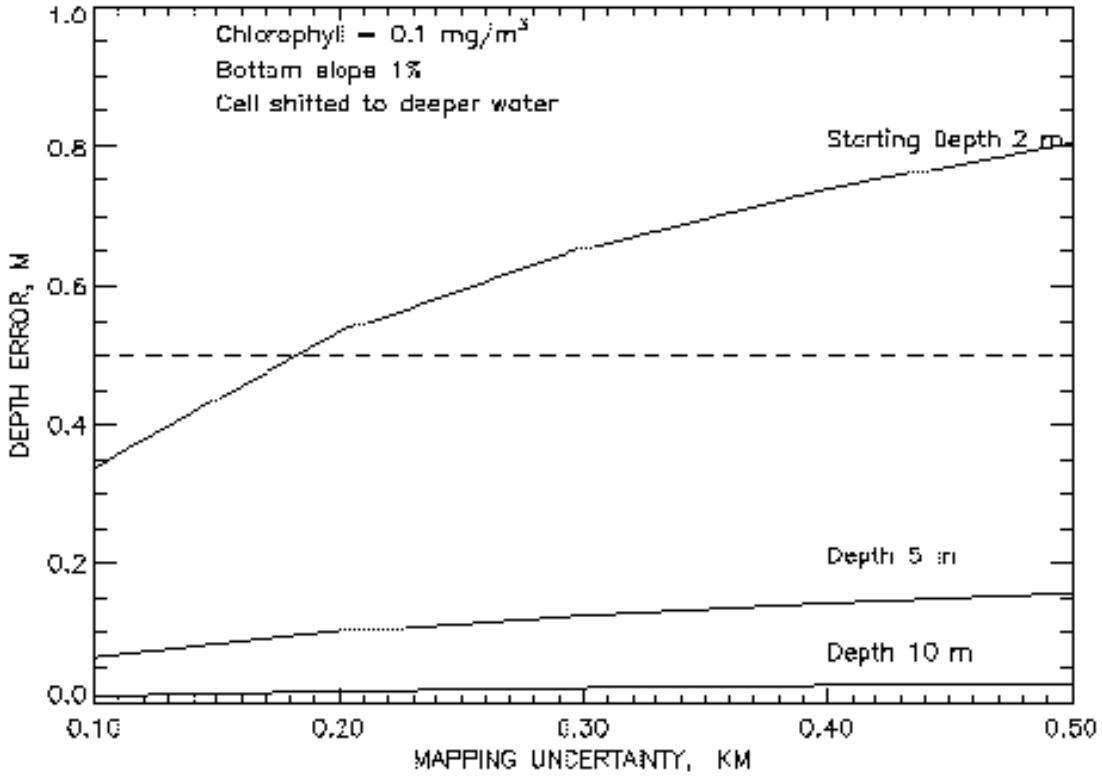

Figure 12. Mapping uncertainty for different starting depths with a chlorophyll value of 0.1 mg/m^3.

Figure 13 displays the change in retrieved bottom depth accuracy due to changes in chlorophyll. The starting depth is 8 m. It clearly shows that, for large true depth changes, the accuracy exceeds the threshold value of 30% except for the case where the chlorophyll concentration is 2.1 mg/m^3. This is true because the increased chlorophyll concentration limits the penetration of light into the waters, thus giving a false bottom.

In the case where the delta true value is 0.5 m, the retrieved bottom depth change accuracy is well within the threshold values. The accuracy error greatly increases as the chlorophyll concentration becomes larger.

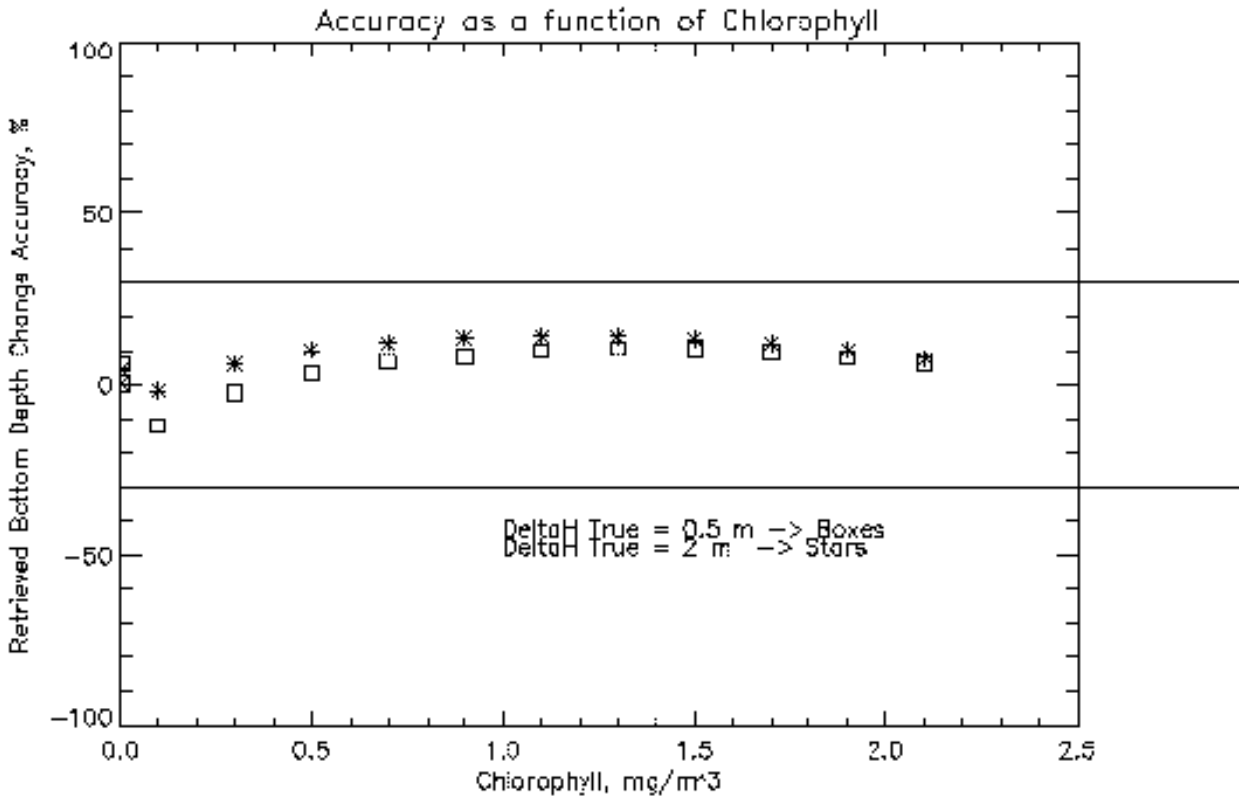

Figure 13. Retrieved bottom depth change accuracy for changes in chlorophyll concentration for a fixed starting depth of 8 m.

In order to understand how the increase in initial depth affects the retrieved bottom depth change accuracy, several studies were done over depths ranging from 5 to 20 m for a chlorophyll concentration of 0.1 mg/m^3 (Figure 14). As the starting depth increases the accuracy error also drastically increases for both the delta true change in depth of 0.05 and 2 m.

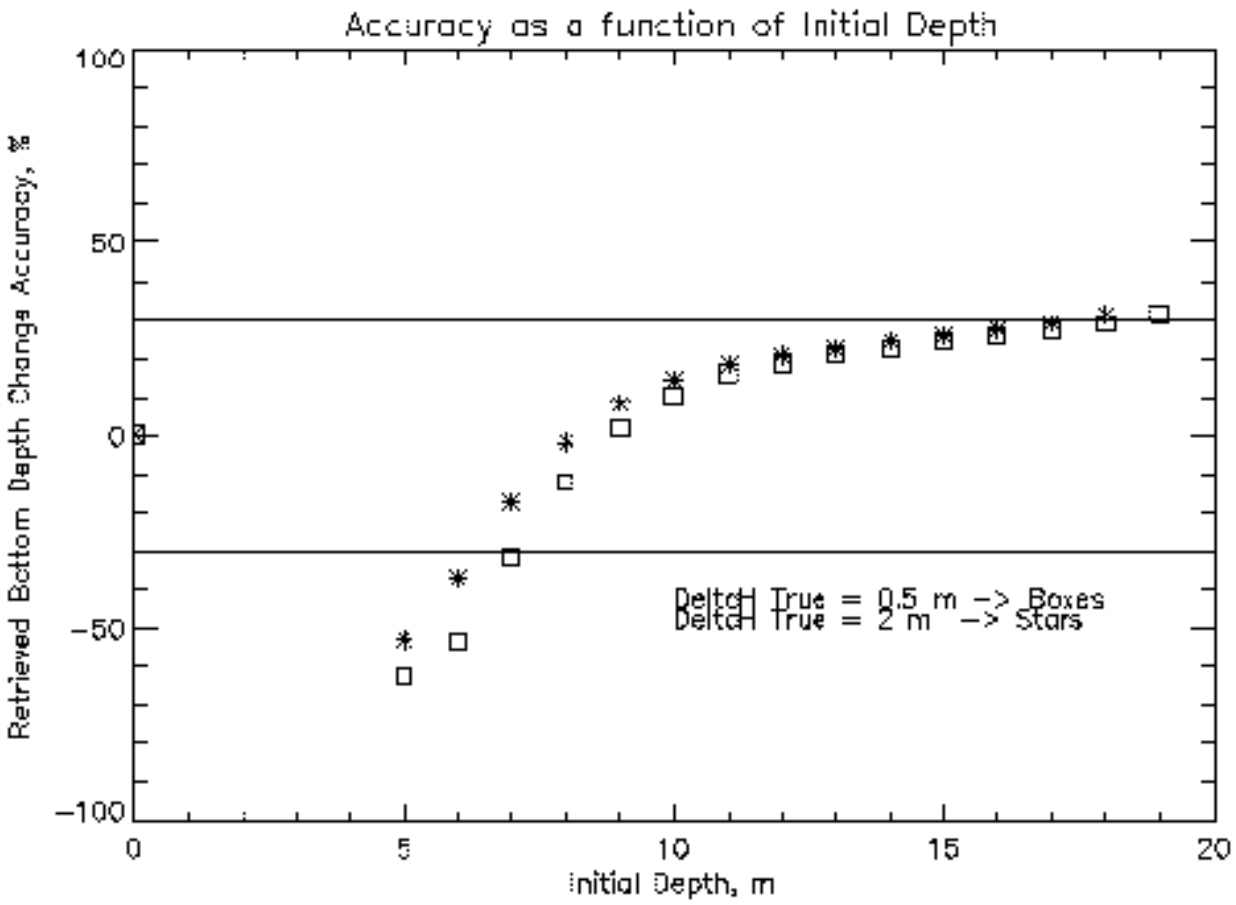

Figure 14. Retrieved bottom depth change accuracy as a function of initial depth for a chlorophyll concentration of 0.1 mg/m^3.

Bahamas Scene

Two days of SeaWiFS LAC Level 1 data were obtained from the GSFC DAAC (refer to Figure 15 and 16). This region was chosen because the current littoral sediment transport algorithm works for shallow flat-bottom ocean regions. The pixels with clear deep water that are closest to the shallow water area were selected. Then, the atmospheric correction of the TOA radiances for those pixels was performed to retrieve values of the atmospheric parameter, $\varepsilon(\lambda, 865)$. These values of $\varepsilon(\lambda, 865)$ were extended for the whole shallow water area. The atmospheric correction was performed for the shallow water area to retrieve the remote sensing reflectance in bands at 555 and 672 nm. Figure 17 displays the difference of the relative change in TOA reflectance at 555 nm for the image pair.

From the remote sensing reflectance retrieved for the two days, the bottom depth changes during that two-day period were determined. Figure 18 shows the water depth change in meters. Finally, the bottom depth changes was converted to littoral sediment transport and then mapped.

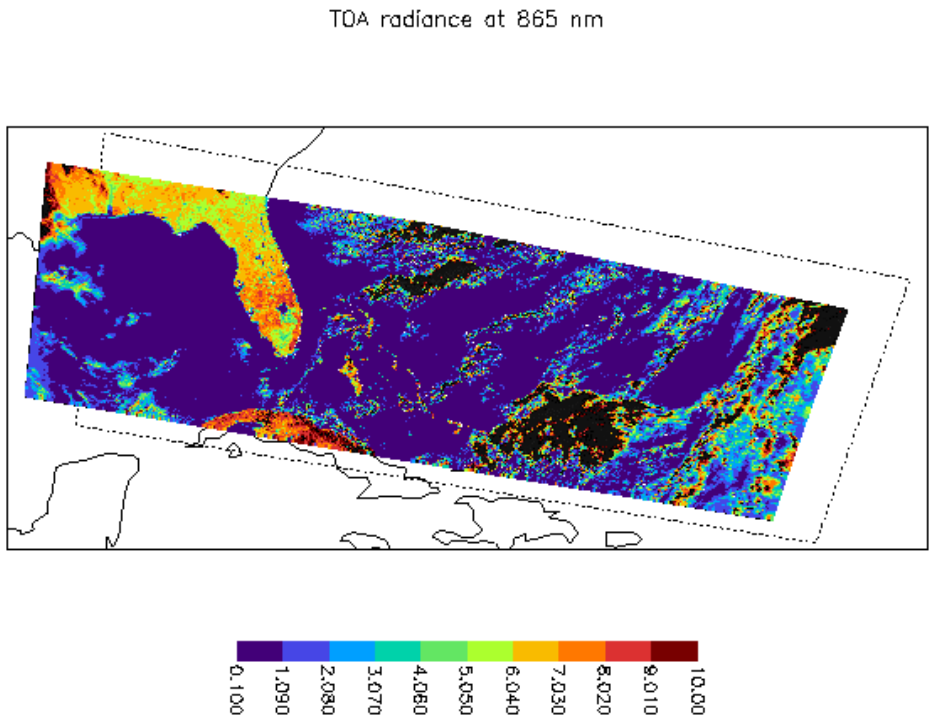

Figure 15. Bahamas Scene TOA Radiance at 865 nm

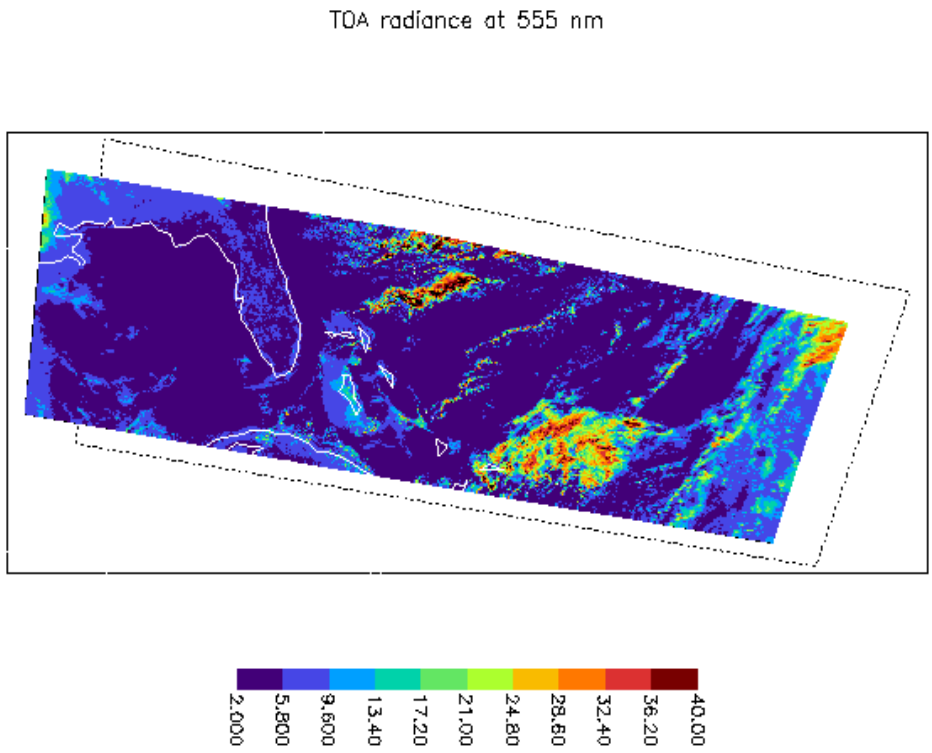

Figure 16. Bahamas Scene TOA Radiance at 555 nm.

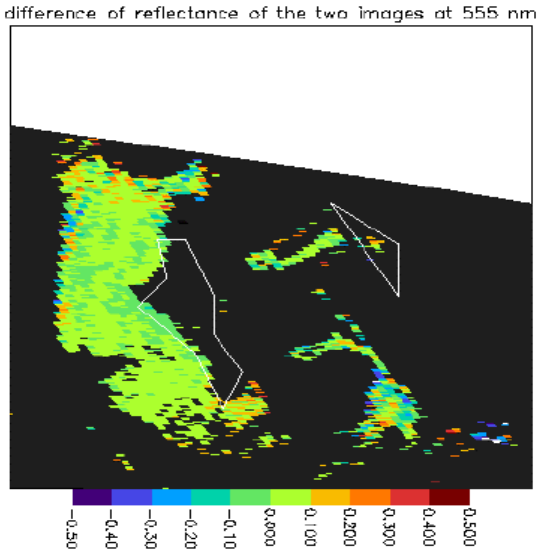

Figure 17. Difference in reflectance of the two images at 555 nm.

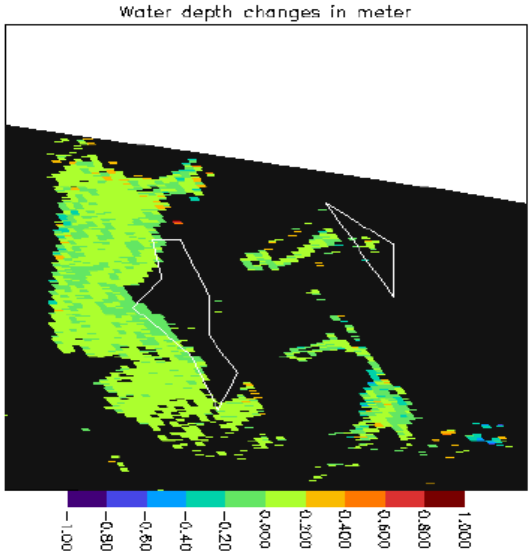

Figure 18. Water depth change in meters.

3.5.2 Sensor Noise Sensitivity Study

The effects of radiometric noise on the precision of littoral sediment transport have been studied using a preliminary semi-analytic model for water-leaving radiances combined with the SBRS noise models (Hucks, 1998). The SRD threshold requirement for precision is the greatest of 40 percent or TBD, and the accuracy is the greater of 30 percent or TBD.

Retrievals were obtained over a range of depths for the different noise models. The average retrieval was unbiased; however, the precision ranged from 0.07 m for a depth of 1 m to 0.25 m at a depth of 10 m for noise model 3. The precision progressively got worse as the noise model number increased.

In order to apply these results to the EDR one has to compare them to typical values for "true" changes in bathymetry. Assuming a 0.30 m change in bathymetry during a storm event, the accuracy ranges from 23.3 percent at 1 m depth to 83.3 percent at 10 m depth.

3.5.3 Sensitivity Study Conclusions

VIIRS sensor performance model 3 has been tentatively recommended as sufficient to meet the LST precision requirement of 20 percent.

3.6 PRACTICAL CONSIDERATIONS

3.6.1 Numerical Computation Considerations

The algorithm is computationally fast and is suitable for operational use.

3.6.2 Programming and Procedural Considerations

The algorithm makes use of an algebraic equation. The computer code is written in FORTRAN. The algorithm parameters are read in from a file.

3.6.3 Configuration of Retrievals

A configuration file is used to establish the numerical values of adjustable parameters used within the retrieval. This avoids specific values in the software and allows for the adjustment of the algorithm to specific ocean areas, such as coastal waters.

3.6.4 Quality Assessment and Diagnostics

A number of parameters and indicators will be reported in the Littoral Sediment Transport Product as retrieval diagnostics. Summaries of these parameters will be reviewed for quality assessment by the VIIRS team. Included among these are parameters of the configuration file and statistical information regarding the processing.

3.6.5 Exception Handling

LST retrievals are performed only if the atmospheric correction algorithm provides positive values of water-leaving radiances in the VIIRS visible bands at 555 and 672 nm. If the algorithm results in bottom depth changes above a predetermined maximum value, then the algorithm outputs will be set to -1.

3.7 ALGORITHM VALIDATION

Validation of the algorithm will rely on in situ measurements of water-leaving radiance and ocean bottom depth in shallow coastal areas.

3.8 ALGORITHM DEVELOPMENT SCHEDULE

An algorithm has been developed to determine the littoral sediment transport EDR for the VIIRS sensor.

4.0 ASSUMPTIONS AND LIMITATIONS

4.1 ASSUMPTIONS

The following assumptions are made with respect to the littoral sediment transport retrievals described in this document.

- Bottom albedo is not changed during two successive measurements made for the retrieval of littoral sediment transport

- Bottom albedo does not affect the red band reflectance, R_5. This means that $[K_d(672)+K_u(672)]h>>1$, where K_d and K_u are the diffuse attenuation coefficients for downwelling and upwelling radiation respectively, and h is the bottom depth.

- Chlorophyll and gelbstoff absorption is negligible at wavelengths 555 and 672 nm. That means the suspended particulate matter is a major seawater constituent in, which variation determines optical properties of seawater and, hence, seawater reflectance and diffuse attenuation of in-water radiation.

- Bottom albedo, R_b, is much greater than the deep seawater diffuse reflectance, R_∞, at wavelengths 555 and 672 nm. This is valid for sandy bottoms, where reflectivity is approximately 20 percent (Lyzenga, 1978).

4.2 LIMITATIONS

The following limitations apply to the littoral sediment transport retrieval described in this document.

- Retrievals will not be performed over a pixel for which atmospheric correction fails, resulting in zero or negative water-leaving radiance in the VIIRS visible bands, 555 and 672 nm.

- Retrievals will not be performed for a pixel if the algorithm results in bottom depth changes above a pre-determined maximum value.

- Flat bottom

- Restricted optical parameter range

- Algorithm does not perform to requirements when highly variable optical properties are utilized.

- Case 2 waters – accuracy decreases

- Restricted depth range

5.0 REFERENCES

Aas, E. (1987). Two-stream irradiance model for deep waters. *Applied Optics*, Vol. 26, 2095-2101.

Burns, R.F. (1998). Sandy Duck 1997: ONR, Corps of Engineers, USGS, others make long-planned major assault on understanding nearshore coastal dynamics processes. *Sea Technology*, 51 – 59.

Cracknell, A.P., M. Ibrahim, and J. McManus (1987). Use of satellite and aircraft data for bathymetry studies. In *Proceedings, Thirteenth Annual Conference of the Remote Sensing Society,* U. Nottingham.

Fryer, J.G. and H.T. Kneist (1985). Errors in depth determination caused by waves in through-water photogrammetry. *Photogramm. Record,* Vol. 11, 745.

Garver S.A., and D.A. Siegel (1997). Inherent optical property inversion of ocean color spectra and its biogeochemical interpretation: 1. Time series from the Sargasso Sea. *J. Geophys. Res*., Vol. 102, 18,607-18,625.

Golubitskiy, B.M., and I.M. Levin (1980). Transmittance and reflectance of layer of highly anisotropic scattering medium. Izvestiya USSR Academy of Sciences, *Atmospheric and Oceanic Physics*, Vol. 16, 926-931.

Gordon, H.R. (1973). Simple calculation of the diffuse reflectance of the ocean. *Applied Optics,* 12, 2803-2804.

Gordon, H.R., O.B. Brown, R.H. Evans, J.W. Brown, R.C. Smith, K.S. Baker, and D.K. Clark (1988). A semianalytic radiance model of ocean color. *J. Geophys. Res*., Vol. 93, 10,909-10,924.

Haltrin, V.I., and G.W. Kattawar (1993). Self-consistent solutions to the equation of transfer with elastic and inelastic scattering in oceanic optics: I. Model. *Applied Optics*, Vol. 32, 5356-5367.

Hoge, F.E., and P.E. Lyon (1996). Satellite retrieval of inherent optical properties by linear matrix inversion of oceanic radiance models: an analysis of model and radiance measurement errors. *J. Geophys. Res.*, Vol. 101, No. C7, 16,631-16,648.

Hucks, J. (1998). RSTX internal memo Y1629.

Lee, Z., K.L. Carder, S.K. Hawes, R.G. Steward, T.G. Peacock, and C.O. Davis (1994). Model for the interpretation of hyperspectral remote-sensing reflectance. *Appl. Opt*., Vol. 33, No. 24, 5721-5732.

Lee, Z., K.L. Carder, C.D. Mobley, R.G. Steward, and J.S. Patch (1998a). Hyperspectral remote sensing for shallow waters. I. A semianalytical model. *Appl. Opt*., Vol. 37, No. 27, 6328-6338.

Lee, Z.P., K.L. Carder, C.D. Mobley, R.G. Steward, and J.S. Patch (1998b). Hyperspectral remote sensing for shallow waters: 2. Deriving depths and optical properties by optimization. submitted to *Applied Optics*.

Lyzenga, D.R. (1978). Passive remote sensing techniques for mapping water depth and bottom features. *Applied Optics*, 17, 379 – 383.

Maritorena, S., A. Morel, and B. Gentili (1994). Diffuse reflectance of oceanic shallow waters: influence of water depth and bottom albedo. *Limnology and Oceanography*, Vol. 39, 1689-1703.

Mobley, C.D. (1995). HYDROLIGHT 3.1 Users' Guide. Final report, SRI (SRI International, Menlo Park, CA 94025) Project 5632, 65 pages.

Morel, A., and L. Prieur, (1977). Analysis of variations in ocean color. *Limnology and Oceanography*, Vol. 22, 709-722.

Morel, A. (1988). Optical Modelling of the upper ocean in relation to its biogenous matter content (Case 1 waters). *J. Geophys. Res*., Vol. 93, 10749-10768.

Philpot, W.D. (1989). Bathymetric mapping with passive multispectral imagery. *Applied Optics,* 28, 1569 – 1578.

Polcyn, F.C. and D.R Lyzenga (1973). Calculations of water depth from ERTS-MSS data. In *Proceedings*, *Symposium on Significant Results from ERTS-1,* NASA Spec. Publ. Sp-327.

Roesler, C.S., and M.J. Perry (1995). *In situ* phytoplankton absorption, fluorescence emission, and particulate backscattering spectra determined from reflectance. *Journal of Geophysical Research*, Vol. 102, 13,279-13,294.

Rosenshein, J.S., C.R. Goodwin and A. Jurado (1977). Bottom configuration and environment of tampa bay. *Photogramm. Eng*., 43, 693.

Tewinkel, G.G. (1963). Water depths from aerial photographs. *Photogramm. Eng*., 29, 1037.

Weidmark, W.C., S.C. Jain, H.H. Zwick, and J.R. Miller (1981). Passive bathymetric measurements in the Bruce Peninsula region of Ontario. In *Proceedings, Fifteenth International Symposium on Remote Sensing of the Environment* (Environmental Research Institute of Michigan, Ann Arbor).

Vasilkov, A.P. (1997). A retrieval of coastal water constituent concentrations by least-square inversion of a radiance model. *Proceedings of the 4th International Conference on Remote Sensing for Marine and Coastal Environments*, Orlando, Florida, 17-19 March 1997, Vol. II, 107-116.

Zaneveld, J.R.V. (1982). Remotely sensed reflectance and its dependence on vertical structure: a theoretical derivation. *Applied Optics*, Vol. 21, 4146-4150.

tidesonline.nos.noaa.gov